Transactions of the KSNVE, 24(3) : 213~218, 2014
http://dx.doi.org/10.5050/KSNVE.2014.24.3.213

한국소음진동공학회논문집 제 24 권 제 3 호, pp. 213~218, 2014
ISSN 1598-2785(Print), ISSN 2287-5476(Online)

[Special Paper]

# Numerical Analysis of Sunroof Buffeting using STAR-CCM+

## STAR-CCM+를 이용한 썬루프 버페팅 유동 소음 해석

Satish Kumar B†, Fred Mendonça*, Ghuiyeon Kim* and Young R Back*
사티쉬 본투·프레드 멘돈카·김 귀 연·백 영 렬

(Received November 26, 2013 ; Revised March 6, 2014 ; Accepted March 7, 2014)

**Key Words** : Aero Acoustic(유동 소음), Cavity Noise(공명 소음), Sunroof Buffeting(썬루프 버페팅), STAR-CCM+, FRET

**ABSTRACT**

CFD flow simulation of vehicles with open sunroof and passenger window help the automotive OEM(original equipment manufacturer) to identify the low frequency noise levels in the cabin. The lock-in and lock-off phenomena observed in the experimental studies of sunroof buffeting is well predicted by CFD speed sweep calculations over the operating speed range of the vehicle. The trend of the shear layer oscillation frequency with vehicle speed is also well predicted. The peak SPL from the CFD calculation has a good compromise with the experimental value after incorporating the real world effects into the CFD model by means of artificial compressibility and damping correction. The entire process right from modeling to flow analysis as well as acoustic analysis has been performed within the single environment i.e., STAR-CCM+.

**요 약**

썬루프 버페팅 소음의 고유특성을 의미하는 속도에 따른 소음강도의 증-감쇠 현상을 살펴보고자, HSM(Hyundai simplified model) 형상에 대해서 유동소음 해석 프로그램인 STAR-CCM+을 통하여 전체 차속 범위에 걸쳐 시험과 비교 검토하였다. 차량 내부의 재질에 따른 압축성 효과 및 감쇠효과는 인공 압축성과 감쇠 보정 기법인 FRET(frequency response test)를 이용하였다. 시뮬레이션 결과는 특정 속도에서 나타나는 소음 강도의 증-감쇠 시험결과를 매우 잘 예측하였으며 최대 SPL 수치도 정확히 예측하였다. 이는 썬루프 개방에 의해 발생하는 전단면에서의 유동 박리 주파수를 유동 소음 해석인 STAR-CCM+가 전 차속에 걸쳐서 매우 잘 예측하고 있음을 나타낸다.

## 1. Introduction

Wind buffeting noise is included in the dominant automotive noise source, and sunroof buffeting creates quite offensive noise by the additional flow excited resonance phenomenon. The resonance phenomenon is usually occurred by the

† Corresponding Author ; Member, CD-adapco
E-mail : satish.bonthu@cd-adapco.com
Tel : +82-2-6344-6527, Fax:+82-2-6344-6501
* CD-adapco

# A part of this paper was presented at the KSNVE 2012 Annual Autumn Conference
‡ Recommended by Editor-in-Chief Weuibong Jung

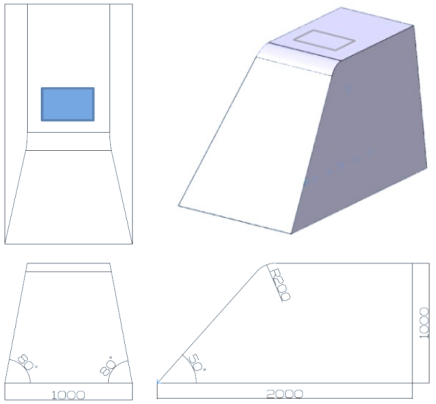


**Fig. 1** Hyundai simple model

coupling of the natural frequency of passenger compartment as well as flow excitation in the shear layer of the vehicle sunroof. CFD acoustic analysis can provide a good insight to understand resonance phenomenon. However the measured natural frequency by experiment and the predicted natural frequency by CFD analysis have always a gap. The gap is originally caused by various characteristics in the vehicle such as absorption materials and leakages. To improve CFD acoustic simulation in terms of accurate natural frequency and lock-in and lock-off phenomena, a new correction method by FRET(frequency response test) was introduced[1].

Current research is focusing on the review of the method and finding additional improvement comparing experimental data. HSM(Hyundai simple model) has been chosen. It is simplified car geometry with sunroof aperture and passenger cabin volume which is kept on the ground as shown in Fig. 1. The CFD result comprised only symmetrical half of the above test geometry for the ease of computations. The simulation geometry considered to be free of leakage.

## 2. Numerical Approach

### 2.1 Mesh Configuration

Geometry is meshed with trimmer(unstructured) model in STAR-CCM+[2] with layered mesh adjacent and normal to the walls for the fine resolution to capture the pressure-gradient induced separation on smoothly curved surfaces. The entire computational domain contains over 5 million cells with finest cell of size 4 mm in the sunroof aperture region as shown in Fig. 2. The mesh is well organized within the domain keeping the finer cells in the aperture and cavity region by the usage of volumetric controls, a tool to refine the mesh in the region of interest. The near-wall mesh resolution in upstream wind tunnel floor and body is constructed to be compatible with the log-law wall function(y+ > 30).

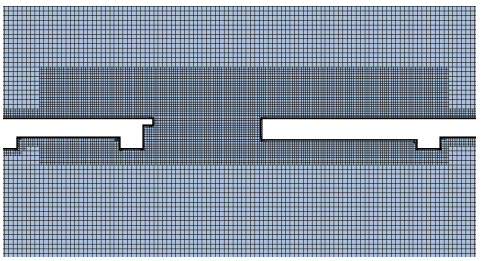

**Fig. 2** Mesh distribution in the aperture region

Mesh refinement studies, not presented here, were conducted by refining the shear layer mesh to 2 mm, and refining the near wall mesh upstream and on the body to a low-Re resolution (y+ ~1). Both refinements confirm the same trends in SPL(dB) and frequency(Hz) versus velocity(kph), with some small improvements.

### 2.2 Simulation Methodology

(1) Governing Equations

The mass and momentum equations are solved in STAR-CCM+ via the finite volume method (FVM) for a general fluid flow in Cartesian tensor notation:

$$\frac{\partial \rho}{\partial t} + \frac{\partial}{\partial x_j}\left(\rho u_j\right) = 0 \tag{1}$$

$$\frac{\partial \rho u_i}{\partial t} + \frac{\partial}{\partial x_j}\left(\rho u_j u_i - \tau_{ij}\right) = -\frac{\partial p}{\partial x_i} \tag{2}$$

Where, $\rho$ = density; $p$ = pressure; $u$ = velocity; $\tau$ = stress tensor; $i, j$ = cartesian coordinate.

(2) Turbulence Modeling

RANS/LES hybrid such as Detached Eddy Simulation has been fairly demonstrated by researchers[3,4] to be suitable for capturing both narrow-band and broad-band flow excitations in high Reynolds numbers fully wall resolved industrial flows. Delayed DES was used for all the cases presented. SST K-Omega Turbulence model is used for RANS part of DES.

(3) Boundary Conditions

Fully compressible ideal gas formulation helps to capture directly the propagation of pressure waves together with flow field. Non-reflective conditions at inflow and outflow boundaries are essential in compressible flows. Reflective boundaries artificially add acoustical resonance in the computational domain which should be avoided.

$$\rho = \frac{p_{abs}}{RT} \tag{3}$$

Where, $p_{abs}$ =absolute pressure; $R$= specific gas constant; $T$= absolute temperature.

(4) Numerics

Second order spatial and temporal accuracy with implicit formulation on unstructured mesh is used. The time step for transient calculations is chosen as 1e-4 sec and 2 seconds of total solution time to ensure a statistically converged time signal.

(5) Process Flow

The schematic of Fig. 3 shows the work flow of the simulation process for sun roof buffeting.

(6) ART VS. FRET

The exact counterpart of acoustic response test(ART) is the virtual frequency response test (FRET). The virtual cabin volume is slightly pressurized and relieved to get its natural frequency and damping characteristic. The pressure decays exponentially in co-sinusoidal fashion

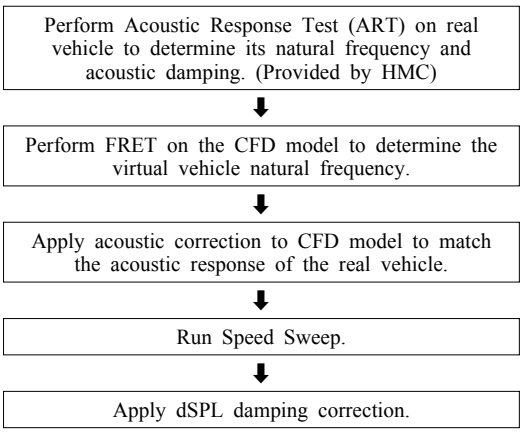


**Fig. 3** Modeling process hierarchy

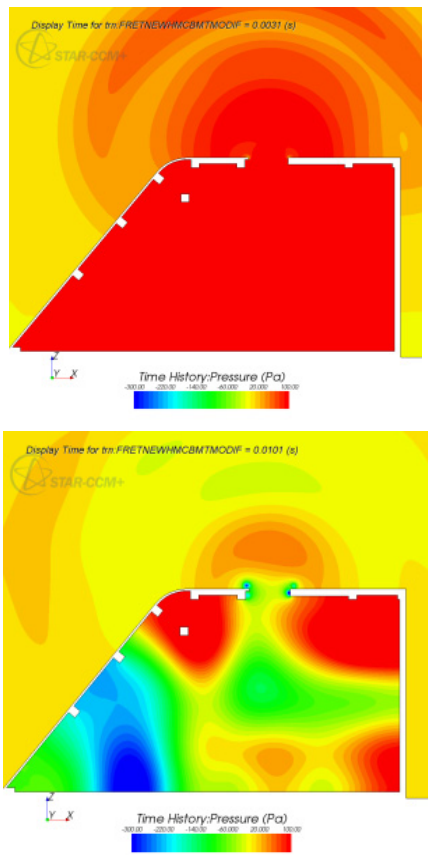


**Fig. 4** FRET pressure distribution initiation and standing wave propagation(left to right)

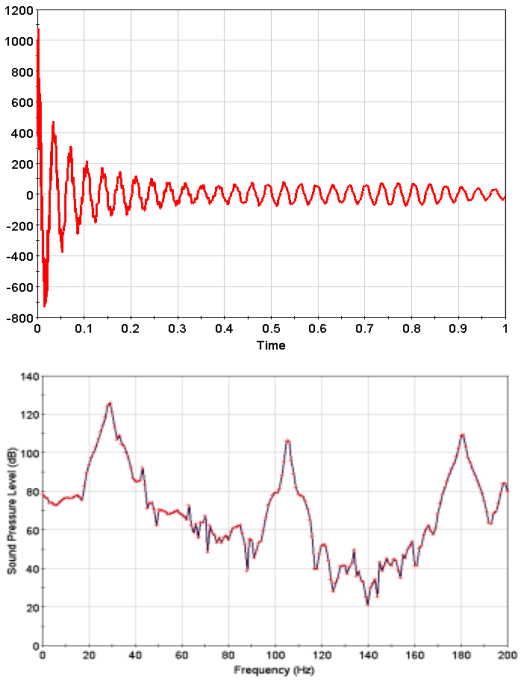


**Fig. 5** FRET pressure-time signal at driver's ear location(left), SPL(dB) (right)

partially propagating to external environment and partially resonates inside the cabin. The resonance represents the natural frequency of the rigid CFD system whereas the pressure decay represents the damping of the virtual system bereft of internal damping, additional leakages(in addition to the sunroof aperture) and compliant walls. We expect negligible numerical damping in the frequency range of interest. Figure 4 shows the imposed pressure distribution inside the cabin and the spherical wave propagation to exterior of the sunroof aperture and creating standing waves in the cabin.

Figure 5 shows the FRET time history of pressure variation at a location inside the cabin representing the driver's ear. The initial decay of the pressure amplitude determines the acoustic damping in the rigid CFD system. It is observed that standing waves are set up at natural frequencies of 29 Hz and 105 Hz.

Figure 6 shows the curve fit approximation of

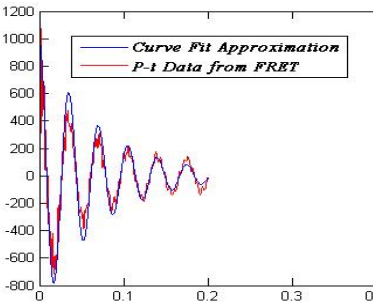


**Fig. 6** Curve fit approximation to the decaying pressure signal from FRET

**Table 1** Comparison of acoustic properties

| Acoustic properties | ART | FRET |
|---|---|---|
| Natural frequency(Hz) | 26.7 | 29 |
| Damping correction(dB) | -3 | |

pressure signal. The acoustic properties of the rigid CFD model compared with the experimental ART properties. Table 1 shows the comparison between ART and FRET.

Table 1 shows the comparison between the acoustic properties of the experimental ART and virtual FRET. The difference between these two gives rise to ideal-to-real vehicle correlations applied as artificial compressibility correction to CFD modeling. Once the idealized CFD system adjusted to the natural frequency of the real system, the pressure decay (β) difference between ideal and real system can be quantified by damping correction (dSPL) and applied to SPL vs. speed curve[1].

$$\mathrm{dSPL} = f(\beta_{\mathrm{ART}}, \beta_{\mathrm{FRET}}, \text{Natural Frequency}) \quad (4)$$

## 3. Speed Sweep Results

Transient simulations were performed at different vehicle speeds ranging from 20 kph to 100 kph. For each speed, simulation was performed for a real time of 2 seconds. The first second simulation is to wash out the effects of the initial

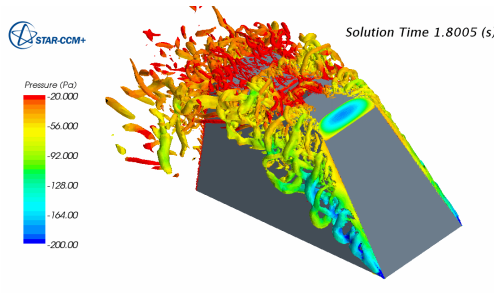


**Fig. 7** Lambda2 iso-surfaces colored by pressure

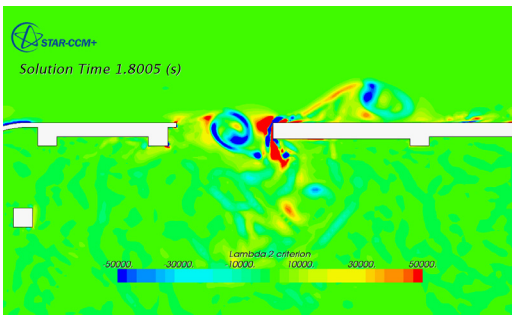


**Fig. 8** Lambda2 contours at the mid plane near the sunroof aperture region

conditions in the flow-field. The following second time data is used for spectral analysis with 2 Hz resolution(hanning windowing, 2 (Pa) blocks with 50 % overlap) where the transient flow achieved statistically steady state condition.

Figure 7 shows the strong interaction of A-pillar turbulent vortices with the edges of the sunroof aperture, creating strong three dimensional features at the edges of the shear layer. However, the central section of the shear layer between A-pillar vortices behaves largely two dimensionally(as shown in Fig. 8).

Figure 8 also shows the convection of the unsteady vortices viewed in the mid plane zoomed into the sunroof aperture region and their interaction with trailing edge of the aperture, partially deflecting the flow into the cabin with its strong introduction of turbulence into the cabin inner volume.

Figure 9 shows the correct trends in SPL vs speed curve prediction, of peak dB maximizing at

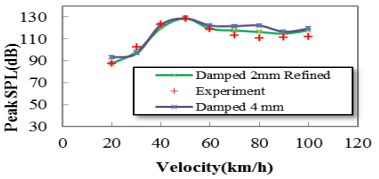


**Fig. 9** Peak SPL vs. speed sweep

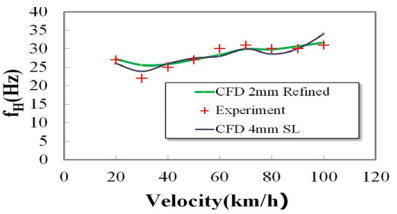


**Fig. 10** Frequency vs. velocity sweep

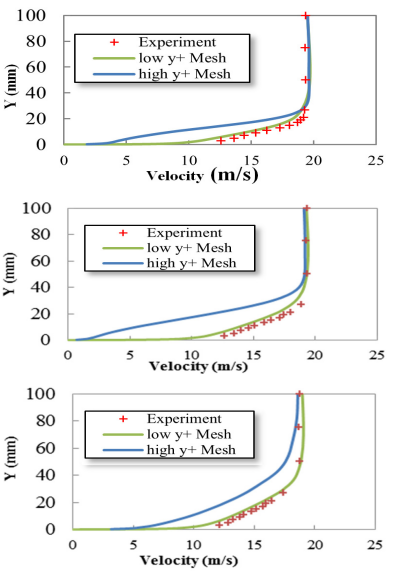


**Fig. 11** BL Velocity profiles at A, B and C

50 kph, with a small dB over-prediction at higher velocities, where improvements are observed when the shear layer mesh is refined to 2 mm. This is due to the fact that the 4 mm refinement of shear layer is not sufficient to capture the fine turbulent scales at high speeds which influence the shear layer mode behavior.

There is no change in the prediction of lock-in and lock-off SPLs and associated velocities even with the shear layer refinement. The linearly in-

creasing trend of frequency with respect to the velocity has been fairly predicted as shown in Fig. 10.

Figure 11 shows the velocity profile at closed roof sections A, B and C; demonstrate correct boundary layer profiles using the low-y+(y+~1) mesh. However, the shear layer behavior is unaffected by the use of a log-law mesh upstream on the wind-tunnel floor and on the body.

## 4. Conclusion

CFD aeroacoustic simulations on HSM with open sunroof have been conducted based on proprietary process of CD-adapco for sunroof buffeting analysis. The lock-in and lock-off phenomena of sunroof buffeting of the vehicle in its operating speed range is well predicted by CFD calculations both in terms of the sound pressure levels as well as the associated shear layer shedding frequency. With smaller mesh size of 2mm compared to 4mm, both simulation results of peak SPL and frequency are quite improved.

## Acknowledgements

Authors are thankful to Hyundai Motors for providing experimental results to validate the CFD predictions.

## References

(1) Mendonça, F., 2013, CFD / CAE Combinations in Open Cavity Noise Predictions for Real Vehicle Sunroof Buffeting, SAE Int. J. Passeng. Cars-Mech. Syst., Vol. 6, No. 1, pp. 360~368.

(2) CD-adapco, 2013, STAR-CCM+ Release 8.04, http://www.cd-adapco.com.

(3) Spalart, P. R., Jou, W. H., Strelets, M. and Allmaras, S. R., 1997 Comments on the Feasibility of LES for Wings, and on a Hybrid RANS/LES Approach, First AFOSR International Conference on DNA/LES, Ruston, Louisiana, USA.

(4) Travin, A., Shur, M., Strelets, M. and Spalart, P., 2002, Physical and Numerical Upgrades in the Detached-eddy Simulation of Complex Turbulent Flows Advances in LES of Complex Flows, Kluwer Academic Publishers, pp. 239~254.

**Satish Kumar Bonthu** received his B.E from Andhra University, Visakhapatnam, India in 2004, M.Tech degree in Engineering Mechanics from IIT Delhi in 2009. He is currently working in CD-adapco as an Engineer. His research interests include aeroacoustics, turbulent flows.

**Fred Mendonça** gained his Masters Degree in 1986 from Imperial College, London, and values 25 years of technical specialism in Computational Fluid Dynamics. He is currently serving as Director, Aeroacoustics Applications in CD-adapco, UK. His research interests include Large Eddy Simulations, aeroacoustics and turbomachinery.

**Ghuiyeon Kim** gained his Masters Degree in the Department of Mechanical and Information Engineering from the University of Seoul in 2005. He is now working as a technical team leader who is responsible to vehicle related simulations including aeroacoustics in CD-adapco Korea.

**Young-Ryoul Back** gained his Ph.D. degree in 1995 from Hanyang University. He is now working as President, CD-adapco Korea. His research interests include CHT analysis, aeroacoustics.